


Quantum phase transitions in the matrix product states of the one-dimensional boson Hubbard model

Min-Chul Cha *Department of Photonics and Nanoelectronics, Hanyang University, Ansan, Gyeonggi-do 15588, Korea*

(Received 31 October 2022; revised 1 December 2022; accepted 6 December 2022; published 14 December 2022)

We study quantum phase transitions in the matrix product states of the one-dimensional boson Hubbard model, whose amount of entanglement is limited by the size of the matrices used in the representation of the states. By measuring entanglement entropy and other physical properties, we observe that the Mott-insulator-to-superfluid transitions occur sharp and continuous, accompanied by shifting transition points that are not blurred by finite entanglement effects. This strongly suggests that the transition always occurs between the Mott insulator and a mean-field-like compressible state, followed by the more entangled superfluid state. Both $O(2)$ and the commensurate-incommensurate transitions are studied, whose properties can be characterized by entanglement spectra and critical exponents.

DOI: [10.1103/PhysRevB.106.235121](https://doi.org/10.1103/PhysRevB.106.235121)

I. INTRODUCTION

Entanglement is a property of quantum systems characterizing the peculiar nature of quantum correlations [1–5], associated with the inseparability between the domains in the formation of a quantum state. It is therefore an interesting question how a limited amount of entanglement modifies this nature and then alters the behavior of quantum phase transitions induced by the divergence of the correlation length. In a restricted region of the Hilbert space accessible, whose area defines the amount of entanglement, a finite length scale, entanglement length, can be introduced that characterizes the range of quantum correlations. It has been argued that the existence of a finite entanglement length modifies the critical properties of quantum phase transitions and results in finite-entanglement scaling behavior [6–8], just as the finite size of the system constraining the correlation length leads to finite-size scaling [9,10]. The matrix product states [11–15] (MPS) provide a very useful tool for realizing quantum systems with a limited amount of entanglement. Here, many-body quantum states are represented in the form of matrix products, the size of which determines the amount of entanglement involved. Numerically, an exact solution will be recovered at the limit where the size of matrix is large enough. Systematic changes in physical quantities near the critical point as a function of entanglement length are expected to produce scaling behaviors. It has been observed that the entanglement length is given in an exponential relation [6,7] $\xi_\chi \sim \chi^\kappa$, where χ is the matrix size, with an exponent κ .

The finite-entanglement scaling behavior of various physical quantities near quantum phase transitions have been found in various one-dimensional systems [6–8,16,17]. However, unlike the finite size effect that smoothes the transition, blurring is seldom found in quantum phase transitions with a finite amount of entanglement. Rather, sharp transitions with shifted transition points appear [7,16], or discontinuous first-order phase transitions are often observed [18,19].

Therefore, it is interesting to investigate whether a finite amount of entanglement has the same effect as the finite size of the system.

In this work, we study the Mott-insulator-to-superfluid quantum phase transition of the one-dimensional boson Hubbard model represented in the MPS. By measuring entanglement entropy and other physical quantities, we explore how the nature of the transition is modified as the size of the matrices changes. We find that the entanglement entropy is very sensitive to quantum mechanical states and changes dramatically near the phase transition. The transition appears continuous and sharp, even with small size matrices. One of the surprising things is that when the transition from the Mott-insulating to the superfluid phases has just occurred, there is an interval in which the entanglement entropy rather decreases and the state exhibits mean-field-like behavior.

II. MPS REPRESENTATIONS

The boson Hubbard model for one-dimensional infinite chains is given by the Hamiltonian

$$H = \frac{U}{2} \sum_i n_i(n_i - 1) - \mu \sum_i n_i - t \sum_i (b_{i+1}^\dagger b_i + b_i^\dagger b_{i+1}), \quad (1)$$

where i is the index for sites, U is the strength of the on-site interaction, t is the hopping amplitude, and μ is the chemical potential. n_i represents the number operator and b_i^\dagger (b_i) denotes the boson creation (annihilation) operator at the i th site. We investigate the superfluid-insulator transition of the system by taking the energy unit $U = 1$ and by tuning μ for a given t , leading to a commensurate-incommensurate (CI) transition in boson density. We also explore $O(2)$ transition by tuning t while keeping the density expectation value fixed at $\langle n \rangle = 1$ for each site by adjusting chemical potential.

A variational ground state of the system is constructed in the canonical form of the MPS wave function [20,21]

$$|\Psi\rangle = \sum_{\{s_i, a_i\}} A_{a_L a_1}^{[s_1]} \Lambda_{a_1} B_{a_1 a_2}^{[s_2]} \Lambda_{a_2} A_{a_2 a_3}^{[s_3]} \cdots B_{a_{L-1} a_L}^{[s_L]} \Lambda_{a_L} \times |s_1, s_2, s_3, \dots, s_L\rangle, \quad (2)$$

where, with $L \rightarrow \infty$ for an infinite chain used in this work, A 's and B 's are the MPS matrices of size $\chi \times \chi$, $a_i = 1, \dots, \chi$ are the bond indices, and s_i are physical indices for the basis states for which we use the number of occupied bosons ($|s_i\rangle = |0\rangle, |1\rangle, |2\rangle, |3\rangle, \dots, |n_{\max}\rangle$) at the i th site. We choose $n_{\max} = 4$, which appears to be big enough to take into account the boson number fluctuations.

In order to find the lowest energy state by using the two-site time-evolving block decimation (TEBD) algorithm [20,21], we construct the wave function by multiplying two sets of matrices A and B alternatively. At each site between the two matrices A and B , the same column vector Λ is multiplied. Its elements, Λ_a , are the Schmidt coefficients, which are non-negative real numbers, ordered such that $\Lambda_1 \geq \Lambda_2 \geq \dots$. In the process of TEBD, we adopt a normalization scheme $\Lambda_1 = 1$. Since Λ_a decreases rapidly as a increases, it is sufficient for practical calculations to choose a finite χ . The limited size χ in the critical region induces a systematic error that reflects the amount of entanglement contained in the ground-state wave function, often leading to predicting scaling behavior as a function of χ . In our study, when choosing χ in our calculation, we take into account whether its value commensurates well with the structure of the entanglement spectrum. As shown below in Fig. 4, in the Mott-insulating phase Λ_a have a structure with a mixture of double and single degeneracy levels.

The half-chain entanglement entropy, S , is a useful quantity to characterize the entanglement properties of a one-dimensional quantum system, which is defined by

$$S = - \sum_{i=1} w_i \log_2 w_i, \quad (3)$$

where w_i are the eigenvalues of the reduced density matrix. Conveniently, in the MPS, w_i are easily obtained as $w_i = \lambda_i^2$, where $\lambda_i = \Lambda_i / \sqrt{\sum_{a=1}^{\chi} \Lambda_a^2}$.

We then use the imaginary TEBD method to determine A , B , and Λ for the ground state by minimizing the energy of the MPS given in Eq. (4). Starting with an arbitrary initial state $|\Psi\rangle$ and proceeding along the imaginary time τ , we obtain the ground state $|\Psi^0\rangle$:

$$\lim_{\tau \rightarrow \infty} e^{-\tau H} |\Psi\rangle \rightarrow |\Psi^0\rangle. \quad (4)$$

By dividing time into small intervals of size $\Delta\tau$, we apply the Suzuki-Trotter decomposition $e^{-\tau H} = (e^{-\Delta\tau H})^N$ ($\Delta\tau = \tau/N$), so that

$$e^{-\Delta\tau H} = \prod_{i=1,3,\dots}^{L-1} e^{-\Delta\tau h_{i,i+1}} \prod_{i=2,4,\dots}^L e^{-\Delta\tau h_{i,i+1}},$$

$$h_{i,i+1} = \frac{1}{2} (h_i^0 + h_{i+1}^0) - t (b_{i+1}^\dagger b_i + b_i^\dagger b_{i+1}),$$

$$h_i^0 = U n_i (n_i - 1) - \mu n_i, \quad (5)$$

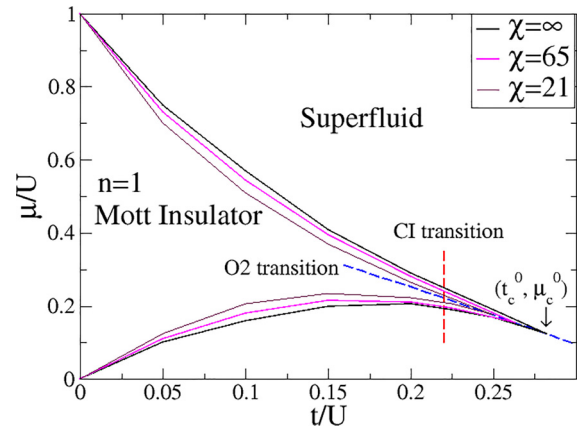


FIG. 1. A schematic phase diagram of the one-dimensional boson Hubbard model for different χ 's. As χ decreases, the Mott insulating phase area is reduced and the phase boundary, not blurred even for small χ , moves inward. This means that the locations of the CI and the $O(2)$ transitions depend on χ , which is different from what we expect from finite size effects.

where we bipartite the system into two parts containing odd and even bonds. The number of repetitions N is determined under the condition that the energy difference in the subsequent state is less than $0.1 - 0.5 \times 10^{-12}$. A small tolerance is essential to distinguish subtle differences in entanglement entropy. If necessary, the TEBD process is extended and repeated more until we reach the state within the tolerance.

Smaller $\Delta\tau$ reduces the decomposition errors, but requires a longer time for the TEBD process. We choose $\Delta\tau = 0.001$ in our calculations, which costs a long time but is necessary to obtain the lowest energy state, especially near the phase transition. In a uniform system, we have

$$e^{-\Delta\tau h_{i,i+1}} |\Psi^0\rangle = e^{-\Delta\tau \varepsilon_0} |\Psi^0\rangle, \quad (6)$$

where ε_0 is the ground-state energy per site.

III. MOTT-INSULATOR-SUPERFLUID TRANSITIONS

We study the quantum phase transitions of the model, represented by the MPS. By measuring the entanglement entropy as well as other quantities such as the density and the single-particle amplitude, we determine the phase boundaries and investigate the critical properties. Figure 1 shows a schematic phase diagram of the model with densities $\langle n \rangle \approx 1$ for different χ 's. For small χ , the Mott insulating phase area decreases and the phase boundary moves inward. The locations of the CI and $O(2)$ transitions depend on χ . This is quite different from what we expect from finite size effects that blur the boundary instead of shifting it. Previously MPS studies for this model have been reported [16]. Our study demonstrates the properties of the phase transition in more detail near the phase transition point and the presence of mean-field-like states. We will discuss these transitions below.

A. $O(2)$ transition

Repulsive interactions between bosons lead to the Mott insulating phases with commensurate densities for small t

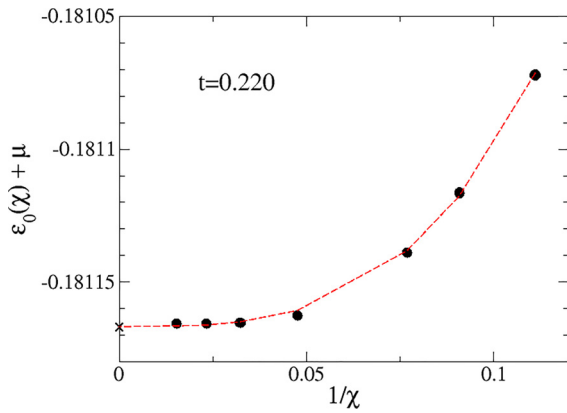


FIG. 2. The scaling behavior of the energy $\varepsilon_0(\chi) + \mu$ in the Mott-insulating phase at $t = 0.220$ as a function of the matrix size χ . In the Mott-insulating phase, the density is fixed at $\langle n \rangle = 1$ so that the chemical potential term just adds a constant $-\mu$ to the total energy. By fitting the curve, we obtain that $\varepsilon_0^* + \mu = -0.181167$ and $\kappa = 1.65(5)$.

as shown in Fig. 1. The quantum correlation length of the MPS represented by a matrix of size χ is limited by the entanglement length $\xi_\chi \sim \chi^\kappa$. We, therefore, expect that the energy per site, $\varepsilon_0(\chi)$, at the ground state with the particle-hole symmetry obeys the scaling relation

$$(\varepsilon_0(\chi) - \varepsilon_0^*) \sim \chi^{-\kappa(d+1)}, \quad (7)$$

where ε_0^* is the value in the limit $\chi \rightarrow \infty$, and $d = 1$ is the spatial dimension. Figure 2 shows the scaling behavior of $\varepsilon_0(\chi)$ in the Mott-insulating phase at $t = 0.220$. Since the density is fixed at $\langle n \rangle = 1$, we plot $\varepsilon_0(\chi) + \mu$ to offset the constant chemical energy term. By fitting the curves, we obtain $\kappa = 1.65(5)$ for the gapped Mott-insulating state. Note that this value is bigger than the theoretical prediction $\kappa = 1.34$ for the model in the critical gapless states, which is given by the formulas [6] $\kappa = 6/[c(\sqrt{12/c} + 1)]$ with the central charge $c = 1$.

The $O(2)$ transition occurs through proliferation of the particle-hole pairs while keeping the density constant. Here, we induce the transition by changing t while we adjust the chemical potential along [16] $\mu(t) = 0.54067 - 1.32850t - 0.53479t^2$ (dotted line in Fig. 1) and slightly tune $\mu(t)$ if needed in the superfluid phase to make the density as close as $\langle n \rangle \approx 1$. It turns out that the half-chain entanglement entropy is an outstanding quantity that clearly exhibits the signature of the transition as shown in Fig. 3. The half-chain entanglement entropy increases smoothly in the Mott-insulating phase as t/U increases, and then drops as soon as the system crosses the $O(2)$ transition point.

The transitions are sharp and continuous for each χ . This implies that the Mott-insulator-to-superfluid transitions with different χ 's are themselves well-defined phase transitions. The discontinuity shown in the figure seems to be a residue because it takes an impractically long time to achieve the lowest energy state near the transition. Another finding is that entanglement is rather reduced in superfluids near the transitions. This is somewhat surprising, as we expect the

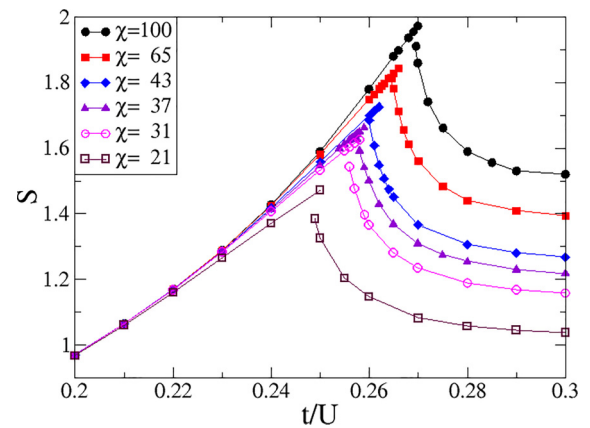


FIG. 3. The half-chain entanglement entropy of the MPS with various χ 's for the $O(2)$ transition of the one-dimensional boson Hubbard model. It exhibits a clear signature of the transition for each χ even though the density stays constant with $\langle n \rangle \approx 1$.

superfluid to occur in a more entangled state. This behavior will be discussed in detail later.

One of the most convenient tools for identifying phases is the spectrum of the reduced density matrix eigenvalues, λ_i^2 , called the entanglement spectrum [22–24]. Figure 4 shows a few λ_i 's in the Mott-insulating and the superfluid phases, starting with the largest at the top. The number of dots represents the degeneracy of the eigenvalues. The hallmark of the Mott-insulating phase is the double degeneracy of the second level (i.e., $\lambda_2 = \lambda_3$), while the first level is singly degenerate, in the entanglement spectrum. Some higher levels are also doubly degenerate. In the superfluid phase, on the other hand, the double degeneracy of some levels are lifted and all levels are singly degenerate. These features suggest that the entanglement spectrum is like a fingerprint that distinguishes phases [19].

Another important property of the entanglement spectrum is the distribution of the eigenvalues. From the eigenvalue

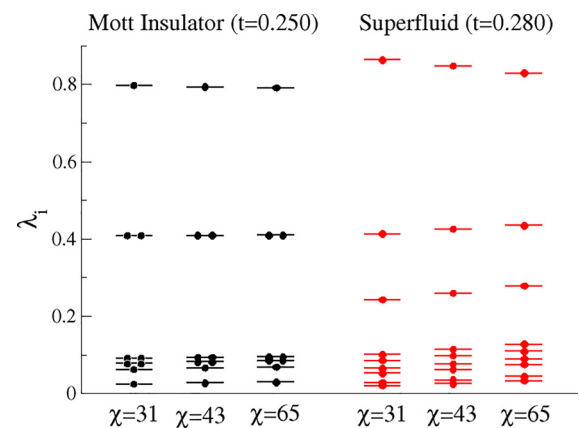


FIG. 4. Some of the largest λ_i 's in the Mott-insulating and the superfluid phases. The number of dots represents the degeneracy of the level. The hallmark of the Mott-insulating phase is that the second level has a double degeneracy, while the first level has a single degeneracy. On the other hand, every level is singly degenerate in the superfluid phase.

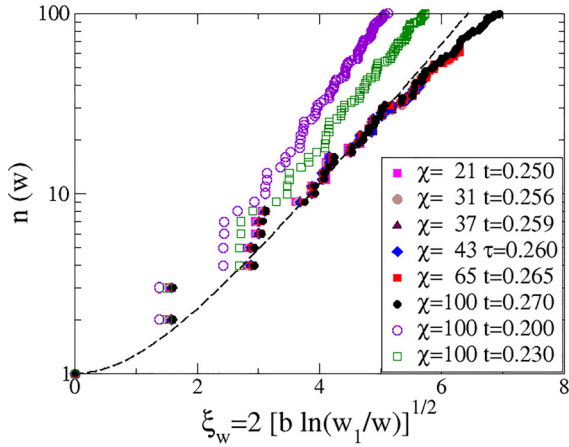


FIG. 5. $n(w)$ represents the mean number of eigenvalues larger than a given w for different χ , obtained at (closed symbols) and off (open symbols) the transition points. The dotted line is the theoretical prediction given by $I_0(\xi_w)$ for the one-dimensional critical systems. At the critical point for each χ , the distributions are consistent with the theoretical prediction. This means that the MPS with different χ have their well-defined transition points.

distribution $P(w) = \sum_i \delta(w - w_i)$, one can define $n(w)$, the mean number of eigenvalues larger than w , as

$$n(w) \equiv \int_w^{w_1} du P(u), \quad (8)$$

where w_1 is the largest eigenvalue. Based on the conformal field theory, it has been proposed that in the one-dimensional critical systems $n(w)$ follows a universal form [25,26]

$$n(w) = I_0(\xi_w), \quad (9)$$

where $I_0(\xi_w)$ is the modified Bessel function of the first kind, $\xi_w \equiv 2\sqrt{b \ln(w_1/w)}$, and $b \equiv \ln(w_1)$. Figure 5 shows $n(w)$ for different χ at (closed symbols) and off (open symbols) transition points. At the transition points, $n(w)$ have the universal form consistent with the theoretical prediction, even though the critical value of t depends on χ . A slight deviation from $I_0(\xi_w)$ when $n(w)$ are large in the samples with large χ appears to be numerical errors where the eigenvalues w_i are extremely small. Also, off the transition points, $n(w)$ obviously does not follow the universal form. This implies that the MPS shift their well-defined critical points as χ changes.

The critical value of the $O(2)$ transition in the thermodynamic limit, t_c^0 , has been studied in many works [27,28]. Here we estimate t_c^0 from $t_c(\chi)$ identified in Fig. 3 for the MPS with finite χ by taking the limit $\chi \rightarrow \infty$. Using an extrapolation, in Fig. 6, we obtain $t_c^0 = 0.280(4)$ as the $O(2)$ transition point in the infinite systems, which is consistent with the previous works [27,28]. Also, the critical value of the chemical potential $\mu_c^0 = 0.127(6)$ can be obtained from t_c^0 along the dotted line in Fig. 1.

B. Commensurate-incommensurate transition

For a given t , by tuning the chemical potential $0 \leq \mu \leq 1$, we induce the CI transitions as shown in Fig. 1. Here, we choose the case where $t = 0.220$. Larger t tends to require very long TEBD processes, whereas for smaller t the χ

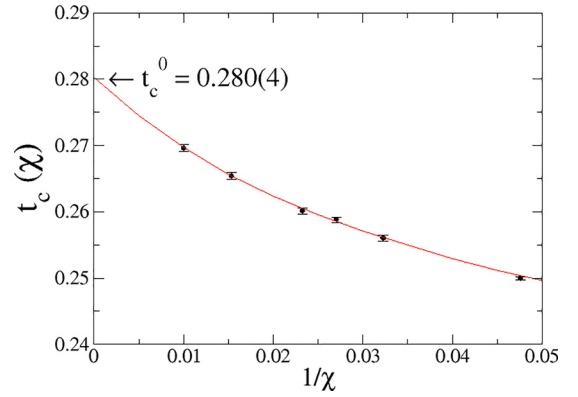


FIG. 6. From $t_c(\chi)$ in Fig. 3 for the MPS with finite χ , the critical value in the limit $\chi \rightarrow \infty$, t_c^0 , is obtained by using an extrapolation.

dependency of $\mu_c(\chi)$, the critical value of the chemical potential for a given χ , seems too weak to analyze the critical behaviors.

Figure 7 shows the half-chain entanglement entropy, density, and single-boson amplitude near the transitions. Again, the transitions appear sharp and continuous without blurring even for small χ . The MPS representation of many-body quantum states is a variational method, so we might end up with many metastable states, especially for large χ and near the transitions. We have tried several different initial states in the TEBD processes until we achieve the lowest energy state whose physical properties runs smoothly with adjacent

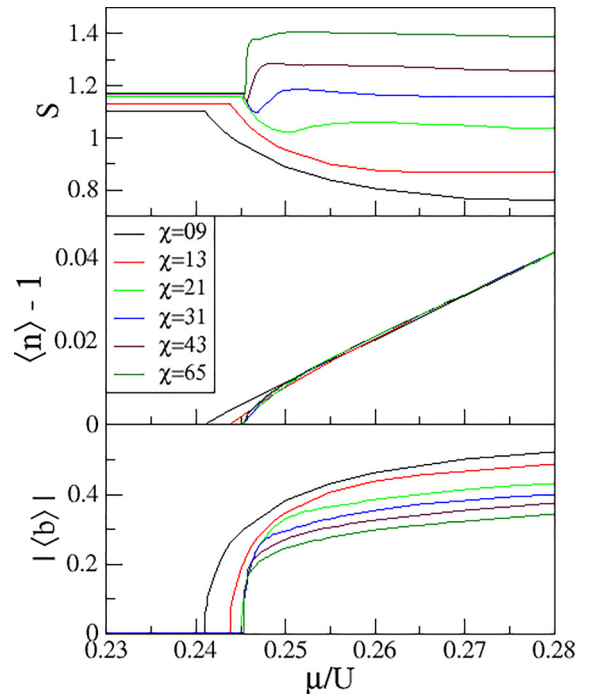


FIG. 7. Half-chain entanglement entropy, density, and single-boson amplitude (top to bottom) induced by tuning the chemical potential are shown. The half-chain entanglement entropy is very sensitive in representing quantum mechanical states, especially near the transitions. The transitions appear continuous and sharp even in the MPS with small χ .

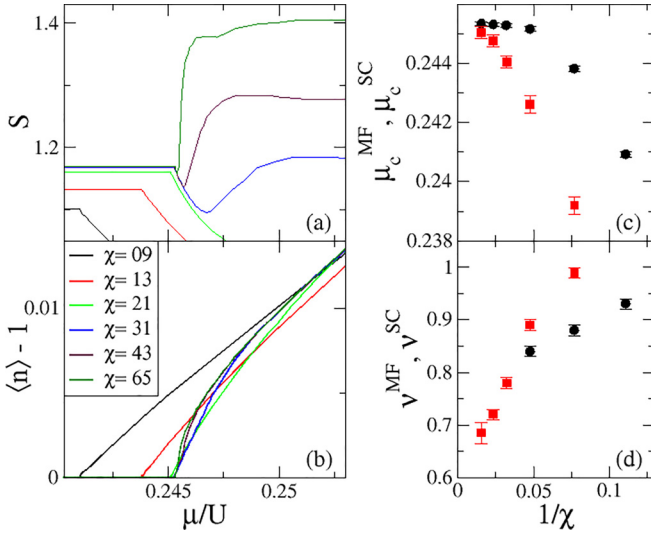


FIG. 8. (a) and (b) are enlarged figures for the behavior of S and $\langle n \rangle - 1$ near the transitions. In the phase transition from the Mott insulator to the superfluid, there is an interval where some mean-field-like (MF) state occurs. Then strongly correlated (SC) state appears as we move further into the superfluid phase. (c) and (d) show the characteristics of the MF and SC states. By fitting the curves of the density in the MF (black circle) and SC (red square) regions, the transition point μ and the correlation length critical exponent ν are obtained.

values. The half-chain entanglement entropy is so sensitive in representing the state that a tiny energy difference can make a big difference. For this reason, in practice, the transitions appear to be of first-order with discontinuities in some physical quantity for systems with large χ , as found in some previous works [18,19]. We believe, however, the discontinuities will eventually disappear in longer TEBD processes since for both small χ and $\chi \rightarrow \infty$ the CI transitions are continuous.

However, if the correlation length is constrained so that it cannot be greater than ξ_χ , continuous phase transitions will turn into crossovers and become blurred, as observed for finite size systems. But this is not the scenario we observe in Fig. 7. In the figure, the transition points are well defined. Moreover, the entanglement entropy decreases in some intervals from the point of transition to the superfluid. This strongly suggests a possibility that the transition occurs between the Mott-insulating state and a (cluster) mean-field-like state [29,30], where the size of the cluster is characterized by ξ_χ .

In order to explore this possibility, we take a closer look at what happens near the phase transition points. Figure 8 is an enlarged plot showing how entanglement entropy and density change near the transition point. We investigate how the density changes in the section where the entanglement entropy sensitively changes. In the Mott-insulating phase, the density remains constant as $\langle n \rangle = 1$. In the compressible superfluid phase, $\langle n \rangle - 1$ arises as a function of μ with different asymptotic behavior depending on χ . For small χ , the density varies almost linearly (mean-field-like behavior) over fairly large intervals. However, as χ increases, there is clearly a crossover into the behavior where the density changes with a smaller exponent as a function of μ (strongly-correlated be-

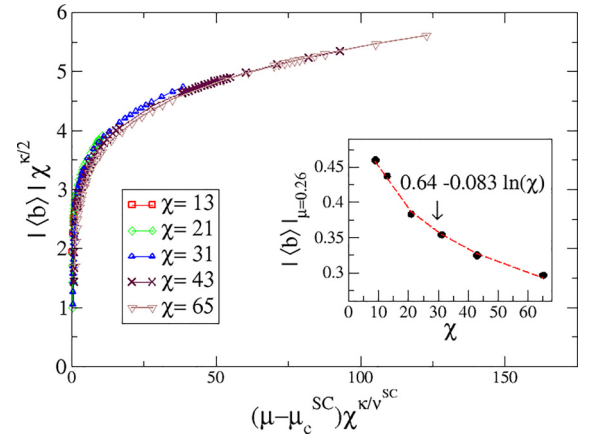


FIG. 9. Scaling behavior of the single-boson amplitude for the strongly correlated states, following a standard scaling ansatz $|\langle b \rangle| \sim \xi_\chi^{-d/2} X((\mu - \mu_c^{\text{SC}}) \xi_\chi^{1/\nu^{\text{SC}}})$, where X is a scaling function, $d = 1$, and $\xi_\chi \sim \chi^\kappa$. Using μ_c^{SC} and ν^{SC} obtained from the asymptotic behaviors in Fig. 8 as fitting parameters, we have a fairly good collapse of the curves with $\kappa = 1.34$. Inset: The amplitude at $\mu = 0.26$ shows a logarithmic dependence on χ .

havior). Interestingly, the mean-field-like behavior occurs as far as the entanglement entropy decreases, and the crossover to the strongly-correlated behavior takes place at the bottom of the valley-shape in Fig. 8(a).

The asymptotic properties of $\langle n \rangle - 1$ can be investigated by fitting the curves in the form

$$\langle n \rangle - 1 = C(\mu - \mu_c)^\nu, \quad (10)$$

where ν is the correlation length exponent, μ_c is an effective transition point for the curves, and C is a constant. The values of the parameters determined by fitting the mean-field-like (MF) and the strongly-correlated (SC) behaviors for given χ are shown in Figs. 8(c) and 8(d). As expected, the correlation length exponent $\nu^{\text{MF}} \rightarrow 1$ as $\chi \rightarrow 1$, the limit of the single-site mean-field approximation. The figure also shows that $\nu^{\text{SC}} \rightarrow 1/2$ as $\chi \rightarrow \infty$, the exact value of the exponent for the generic commensurate-incommensurate transition [31] driven by single-particle excitations. For finite but small χ , the situation is quite analogous to cluster mean-field approximation with the cluster size ξ_χ . The mean-field-like behavior in the MPS has been previously reported in Ref. 18. Our analysis shows that its signature appears as a valley shape of the entanglement entropy with the critical exponents approaching to the mean-field critical exponent as χ decreases.

It is an interesting question whether a physical quantity such as the single-boson amplitude in Fig. 7 exhibits scaling behavior in the region of strongly-correlated states. Figure 9 shows the analysis of this behavior following a standard scaling ansatz

$$|\langle b \rangle| \sim \xi_\chi^{-d/2} X((\mu - \mu_c^{\text{SC}}) \xi_\chi^{1/\nu^{\text{SC}}}) \quad (11)$$

with a length scale $\xi_\chi \sim \chi^\kappa$, where X is a scaling function and $d = 1$ is the spatial dimension. We use the exponent $\kappa = 1.34$, the value based on the conformal field theory (CFT) calculation [6], and the parameters μ_c^{SC} and ν^{SC} obtained from

the asymptotic behaviors in Fig. 8. The figure shows a fairly good collapse of the curves for different χ onto a single curve.

Furthermore, since $X(0) = 0$ (i.e., the superfluid order parameter vanishes at the critical point), in the limit $(\mu - \mu_c^{\text{SC}})^{\xi/\nu^{\text{SC}}} \ll 1$, we expect

$$|\langle b \rangle| \sim (\mu - \mu_c^{\text{SC}})^{\nu^{\text{SC}}/2} [a_0 + a_1 \ln(\chi)]. \quad (12)$$

This form guarantees the expected behavior $|\langle b \rangle| \sim (\mu - \mu_c^{\text{SC}})^{\nu^{\text{SC}}/2}$ near critical point. Then, with a finite μ in the superfluid phase, the amplitude has a logarithmic dependence on χ as shown in the inset.

IV. SUMMARY

We study the quantum phase transition in the matrix product states of the one-dimensional boson Hubbard model, where the amount of entanglement is limited by the size of the matrix, χ , used to represent the states. In order to obtain the lowest energy state, we optimize this variational MPS by using the two-site TEBD method. It turns out that entanglement entropy is a very sensitive tool for representing state properties near phase transitions.

We find that the Mott-insulator-to-superfluid transition occurs sharp and continuous without being blurred by the finite

entanglement effects with the shift of the transition points. From the χ dependence of the transition points, we obtain $t_c^0 = 0.280(4)$ and $\mu_c^0 = 0.127(6)$ for the critical values of the $O(2)$ phase transition. The entanglement spectra follow a universal form at each χ dependent $O(2)$ transition point. In the superfluid phase where the transition just occurs, an interval in which the entanglement entropy dramatically decreases and then increases, forming a valleylike shape, is observed. As χ increases, this valley becomes narrower and shallower. By analyzing the critical exponent of the density, we argue that the behavior in the decreasing part of the valley is governed by a mean-field-like nature. This means that in the MPS where the amount of entanglement is finite, the quantum phase transition between the Mott insulator and the superfluid always occurs through a mean-field-like compressible state.

ACKNOWLEDGMENTS

The author greatly appreciates useful discussions with M.-H. Chung and J.-W. Lee. This work was supported by the National Research Foundation of Korea (NRF) grant funded by the Korea government (MSIT) (No. NRF-2019R1F1A1062704).

-
- [1] L. Amico, R. Fazio, A. Osterloh, and V. Vedral, *Rev. Mod. Phys.* **80**, 517 (2008).
 - [2] R. Horodecki, P. Horodecki, M. Horodecki, and K. Horodecki, *Rev. Mod. Phys.* **81**, 865 (2009).
 - [3] P. Calabrese, J. Cardy, and B. Doyon, *J. Phys. A* **42**, 500301 (2009).
 - [4] J. Eisert, M. Cramer, and M. B. Plenio, *Rev. Mod. Phys.* **82**, 277 (2010).
 - [5] N. Laflorencie, *Phys. Rep.* **646**, 1 (2016).
 - [6] F. Pollmann, S. Mukerjee, A. M. Turner, and J. E. Moore, *Phys. Rev. Lett.* **102**, 255701 (2009).
 - [7] L. Tagliacozzo, T. R. de Oliveira, S. Iblisdir, and J. I. Latorre, *Phys. Rev. B* **78**, 024410 (2008).
 - [8] B. Pirvu, G. Vidal, F. Verstraete, and L. Tagliacozzo, *Phys. Rev. B* **86**, 075117 (2012).
 - [9] M. E. Fisher and M. N. Barber, *Phys. Rev. Lett.* **28**, 1516 (1972).
 - [10] J. Cardy, *Finite-Size Scaling* (Elsevier, Amsterdam, 1988).
 - [11] R. Orús, *Ann. Phys.* **349**, 117 (2014).
 - [12] U. Schollwöck, *Ann. Phys.* **326**, 96 (2011).
 - [13] D. Perez-Garcia, F. Verstraete, M. M. Wolf, and J. I. Cirac, *Quantum Inf. Comput.* **7**, 401 (2007).
 - [14] I. P. McCulloch, *J. Stat. Mech.: Theory Exp.* (2007) P10014.
 - [15] G. Vidal, *Phys. Rev. Lett.* **91**, 147902 (2003).
 - [16] M. Pino, J. Prior, A. M. Somoza, D. Jaksch, and S. R. Clark, *Phys. Rev. A* **86**, 023631 (2012).
 - [17] H. Wang, Y. H. Su, B. Liang, and L. Chen, *Eur. Phys. J. B* **88**, 26 (2015).
 - [18] C. Liu, L. Wang, A. W. Sandvik, Y.-C. Su, and Y.-J. Kao, *Phys. Rev. B* **82**, 060410(R) (2010).
 - [19] M.-C. Cha, *Phys. Rev. B* **98**, 235161 (2018).
 - [20] G. Vidal, *Phys. Rev. Lett.* **93**, 040502 (2004).
 - [21] G. Vidal, *Phys. Rev. Lett.* **98**, 070201 (2007).
 - [22] H. Li and F. D. M. Haldane, *Phys. Rev. Lett.* **101**, 010504 (2008).
 - [23] F. Pollmann, A. M. Turner, E. Berg, and M. Oshikawa, *Phys. Rev. B* **81**, 064439 (2010).
 - [24] I. Peschel and V. Eisler, *J. Phys. A* **42**, 504003 (2009).
 - [25] P. Calabrese and A. Lefevre, *Phys. Rev. A* **78**, 032329 (2008).
 - [26] V. Alba, P. Calabrese, and E. Tonni, *J. Phys. A* **51**, 024001 (2018).
 - [27] K. V. Krutitsky, *Phys. Rep.* **607**, 1 (2016).
 - [28] T. G. Kiely and E. J. Mueller, *Phys. Rev. B* **105**, 134502 (2022).
 - [29] D. Pekker, B. Wunsch, T. Kitagawa, E. Manousakis, A. S. Sørensen, and E. Demler, *Phys. Rev. B* **86**, 144527 (2012).
 - [30] D.-S. Lühmann, *Phys. Rev. A* **87**, 043619 (2013).
 - [31] M. P. A. Fisher, P. B. Weichman, G. Grinstein, and D. S. Fisher, *Phys. Rev. B* **40**, 546 (1989).